Ziziphus Spina Christi Leaves Methanol Extract Evaluation as Antifungal, Antibacterial, Antioxidant and Green Inhibitor for Carbon Steel Alloy Corrosion in Hydrochloric Acid

Sarah Z. Al-Ashoor, Dawood S. Ali and Hadi Z. Al-Sawaad*

University of Basra, College of Science, Department of Chemistry, Basra, Iraq
*Corresponding author: hadi.ziara@uobasrah.edu.iq

Received 22/10/2021; accepted 02/02/2022
https://doi.org/10.4152/pea.2023410205

Abstract
In this study, Zs-c leaves were extracted by a 70% CH_3OH solvent. The extract was investigated as green corrosion inhibitor for CS C1010 alloy in 0.1 M HCl. The study was done with different inhibitor concentrations (1, 2, 8 and 9 ppm). The extract showed the highest IE of 96.06%, at 9 ppm. The inhibitor adsorption on the CS alloy surface was found to obey the Langmuir's adsorption isotherm model. K_{ads}, ΔH_{ads}, ΔS_{ads} and ΔG_{ads} were also calculated. The temperature effect on Zs-c leaves extract IE%, with the optimal concentration of 9 ppm, was studied at 35,45 and 55 ºC. The results showed that IE% decreased with raising solution temperatures. In addition, E_a^*, ΔH, ΔS and ΔG kinetic parameters were calculated. On the other hand, phytochemical tests and quantitative analysis, such as TPC and TFC, were also carried out. In addition, the anti-bacterial activity or growth inhibition of bacterial strains, such as Ec and Sa, were studied. Anti-fungal activity or growth inhibition studies of Ca and An species were also carried out, at a 100 mg/mL concentration. Anti-oxidant activity was also investigated by DPPH, at concentrations of 100, 250, 500, 750 and 1000 µg/mL, and good results were obtained.

Keywords: *Zs-c* leaves, corrosion inhibitors, phytochemicals, DPPH, Ec, Sa, Ca and An.

Introduction•

Zs-c, commonly known as Christ's Thorn or Jerusalem-thorn, in English, and *Sidr*, in Arabic, is a deciduous tree that is native to warm temperate and subtropical areas, including North Africa, South Europe, Mediterranean, Australia, tropical America, South and East of Asia and Middle East. It belongs to the *Rhamnaceae* family, in the order of Rosales, which contains about 60 genera and more than 850 species. The Zs-c genus consists of about 100 species of evergreen trees and shrubs throughout the world. Zs-c is one of the plants used as herbal medicine. It has been used in traditional Chinese Medicine to treat different diseases, such as digestive disorder, fatigue, liver disease, obesity, urinary problems, diabetes, skin infections, loss of appetite, fever, pharyngitis, bronchitis, anemia, diarrhea, insomnia and cancer. Its leaves contain betulinic and seanotic acids, various flavonoid compounds, saponins, tannins, tritepenoids,

•The abbreviations and symbols lists are in pages 180-181.

phenolics and flavonoids, which have anti-oxidant, anti-inflammatory, anti-microbial, and anti-fungal biological benefits [1-4].
Extracts from plants have been used as green inhibitors, since they are environmentally friendly, non-toxic, cheap and abundantly available [5-8].
Metals and alloys corrosion, particularly in acidic media, is a major industrial problem [9]. It is a naturally occurring phenomenon that deteriorates a metallic material or its properties, because of an environmental reaction. It can cause dangerous and expensive damage to everything from pipelines, bridges and public buildings to vehicles, water and wastewater systems, and even home appliances. Thus, corrosion is one of the most serious problems in the industry, especially in the oil and gas sectors [10]. Most of the corrosion inhibitors are organic compounds containing heteroatoms, such as O, N or S, and multiple bonds that allow their adsorption onto metal surfaces. The inhibitors adsorption depends on the nature of their functional groups and on the electron density at the donor atoms [11].
Approaches available for controlling corrosion include the application of protective coatings to metal surfaces or their treatment, alteration of alloys chemistry and the addition of chemical species to the environment. Recent trends in research include developing environmentally friendly inhibitors, accurately predicting the service life of structures, and finding ways to take advantage of corrosion (such as dealloying) [12].

Materials and methods

Plant material

In October 2020, Zs-c leaves were bought from the local market, well washed and dried, grinded to a fine powder, by an electric mill, and saved in a dry bottle, at 25 ºC.

Zs-c CH_3OH extract preparation

25 g Zs-c leaves powder were prepared by the maceration method [13]. Then, they were added to CH_3OH (70%) as a solvent (200 mL), for 72h, at 25 ºC, with occasional stirring. Afterwards, the liquid was collected, filtered using Whatman's no. 41 filter paper, and evaporated to dryness, under a rotary evaporator, at 40 ºC, in order to obtain the Zs-c CH_3OH crude extract that was kept in dark glass bottles, at 4 ºC, before being analyzed.

Phytochemicals analysis

Chemical tests were carried out on the CH_3OH extract, by using standard procedures, for identifying its constituents, from characteristic color changes [14-18].

Antioxidant activity

DPPH solution preparation

DPPH solution (0.04 mg/mL) was made by weighing 2 mg of the substance and dissolving it in 50 mL CH_3OH, in a measuring flask.

Sample solutions preparation

A stock solution of Zs-c leaves was diluted using CH_3OH, at various concentrations.

Anti-oxidant capacity measurements

First, 2 mL DPPH were mixed with 3 mL CH_3OH, incubated at 25 ºC, for 30 min. The blank anti-oxidant capacity was measured at the maximum wave-length of 517 nm. Then,

the Zs-c leaves CH_3OH extract was prepared for the anti-oxidant capacity measurements, by piping 1 mL of the sample solution, at 100, 250, 500, 750 and 1000 µg/mL. Afterwards, 2 mL DPPH and 2 mL CH_3OH were added to the above concentrations. They were incubated for 30-60 min, at 25 ºC. The extract antioxidant capacity was quantitatively calculated by the measured absorbance, which showed a wave-length of 517 nm. If the color would change from purple to pale yellow, that would confirm the extract anti-oxidant capacity [19].

Anti-bacterial and anti-fungal activities

Two types of bacteria, negative and positive for Gram stain (Ec and Sa), were previously isolated and identified by another work. Muller-Hinton agar medium was used for the bacteria growth plates that were incubated at 37 ºC, for 24 h. The Zs-c leaves CH_3OH extract (100 mg/mL) anti-bacterial activity was evaluated by the disc method. The extract was allowed to diffuse, and then incubated at the same temperature, for 18-24 h. The zone of growth inhibition was measured and recorded in mm [20].

The extract anti-fungal activity was assayed through An and Ca fungi screening, by the diffusion technique, on a PDA growth medium [21]. The fungal suspension was standardized to 106 conidia/mL, in a sterile saline solution (0.85%). 100 µL of each fungal suspension were spread onto the Petri dishes surface. After 10 min of rest, 6 mm diameter holes were punched and filled with 50 or 100 µL of the previously prepared extract samples.

As control samples for each experiment, DMSO and HE acids and TEB (Folicur® 20EC) fungicide solutions were used, at 70% and 0.1%, respectively. Subsequently, the plates were incubated at 28 ± 2 ºC. Each extract was evaluated 3 times, after 72 h, by measuring the fungi mycelial growth inhibition diameter (clear zones were considered indicative of anti-fungal activity).

TPC estimation

The extract TPC was determined by the FCR method, adapted from [22]. In a 100 mL volumetric flask, 200 µL of each extract were mixed with 10% 1.5 mL FCR reagent. The mixture was stirred and allowed to stand for 6 min, before the addition of 7.5% 1.5 mL (w/v) Na_2CO_3. Then, the solutions were mixed with distilled water, for obtaining a final volume of 100 mL. The reaction mixture was immediately homogenized, and kept in the dark, for 90 min, at 25 ºC.

The absorbance reading of each solution was determined at 765 nm, with a UV-vis spectrophotometer. A calibration curve was performed by adopting the same operating procedure, and using $C_7H_6O_5$ as positive control. The total phenolic concentrations of each extract were calculated from the linear regression equation of the calibration range established with GA. The results were expressed in mg GAE/g of the dry plant.

TFC estimation

The flavonoids were quantified by direct dosing with $AlCl_3$, according to a method adapted from [23]. In a 50 mL volumetric flask. 100 mL of each extract were mixed with 20 mL distilled water. After 5 min, 100 mL 10% (m/V) $AlCl_3$ were added. The

solutions were then adjusted to 50 mL, with pure CH_3OH, immediately homogenized, and then kept in the darkness, for 30 min, at 25 ºC.
The absorbance of each solution was determined at 433 nm, with a UV-Vis spectrophotometer. A calibration curve was performed by adopting the same procedure, and QCT was used as a positive control.
The flavonoid concentrations of each extract were calculated from the regression equation of the calibration range established with QCT. The results were expressed in mg QCTE/g of the dry plant.

WE preparation
CS alloy strips with the dimensions of 5 x 1 x 0.1 cm were used, with a total area of 11.1 cm^2. The strips were immersed in the solution, and then ground with increasing grades of silicon carbide paper to different smoothness levels (80, 120, 200, 400 and 600). Afterwards, they were washed with distilled water, ethanol and acetone, dried and stored in a dry place at 25 ºC, and placed in desiccators containing silica gel, for protection from moisture [24].

Sample composition
The CS alloy constituents are summarized in Table 1.

Table 1. CS alloy composition.

C%	Mn%	P%	S%	Cu%	Si%	Cr%	As%	Ni%	Fe%
0.13	0.30	0.05	0.04	0.30	0.37	0.10	0.08	0.30	Balance

Electrochemical cell
The electrochemical cell used for the corrosion test in the present study consisted of a 100 mL vessel connected with three electrodes arranged as follows: Pt, CS and SC as CE, WE and RE, respectively.

PDP studies (Tafel plots)
This technique is commonly employed for measuring corrosion resistance, and j *vs*. E, through OCP set up, for 20 min. The polarization curve was acquired by scanning in the potential range from -250 to + 250 mV *vs*. OCP, using a computer to control a potentiostat/galvanostat, at a SR of 10 mV/s^{-1}.

Solutions preparation
The prepared compounds were individually synthesized with different concentrations (1, 2, 8 and 9 ppm), at 298 K. Then, the optimal concentration was studied at different temperatures (308, 318 and 328 K), in HCl.

Results and discussion
Phytochemicals analysis
Phytochemical screening for Zs-c leaves CH_3OH extract revealed the presence of flavonoids, phenols, carbohydrates, tannins, saponins, alkaloids, fixed oils and fats, as summarized in Table 2.

Table 2. Phytochemical analysis of Zs-c leaves CH_3OH extract.

Phytochemical analysis	Flavonoids	Phenols	Saponins	Alkaloids	Carbohydrates	Tannins	Fixed oils and fats
Zs-c leaves CH_3OH extract	+++	+++	+++	++	++	++	++

Zs-c leaves CH_3OH extract phytochemical analysis results shown in Table 2 revealed a positive detection of all the tested phytochemicals.

Antioxidant activity

Free radicals that are commonly used as a model for assessing inhibitors anti-oxidant activity include DPPH, a stable compound, with absorbance values in the range from 510 to 520 nm [25]. This method is based on the (Diphenyl picryl hydrazine) DPPH free radical reduction in a colored solution, by its inhibition. When the DPPH in the purple solution meets the electron donor material it is reduced, and its color is replaced by yellow, from picryl group [26]. The inhibitor anti-oxidant activity was measured by a UV-vis spectrophotometer, at a wavelength of 517 nm, as the DPPH solution maximum wavelength [27], and its strength was indicated by the IC_{50} value. IC_{50} values lower than 100 µg/mL are said to have strong anti-oxidant activity that is able to inhibit 50% of the oxidation. Since the result of the IC_{50} value was 62.89 µg/Ml, it can be stated that Zs-c leaves extract anti-oxidant activity was strong. $C_7H_6O_5$ positive control showed a higher IC_{50} (97.47 µg/mL). Table 3 shows the scavenging activity of Zs-c leaves CH_3OH extract on DPPH, and IC_{50} value.

Table 3. Scavenging activity of Zs-c leaves CH_3OH extract on DPPH.

Extract	Concentrations (µg/mL)	Scavenging activity CH_3OH	Scavenging activity $C_7H_6O_5$
Zs-c leaves in CH_3OH	100	48.89	51.84
	250	56.90	62.59
	500	75.44	79.66
	750	84.51	91.57
	1000	87.67	96.83
	IC_{50}	62.89	2.16

Figs. 1 and 2 show the scavenging activity of Zs-c leaves CH_3OH extract on DPPH.

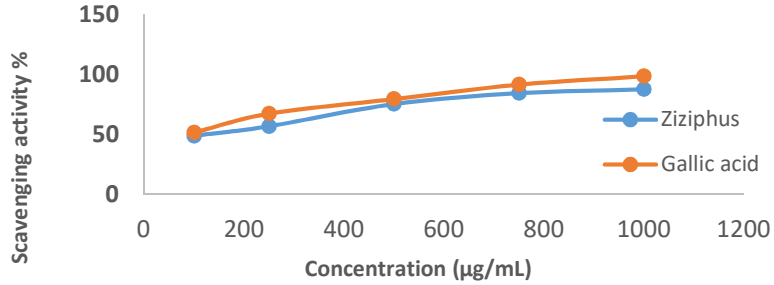

Figure 1. Scavenging activity of Zs-c leaves CH_3OH extract and $C_7H_6O_5$ on the DPPH radical.

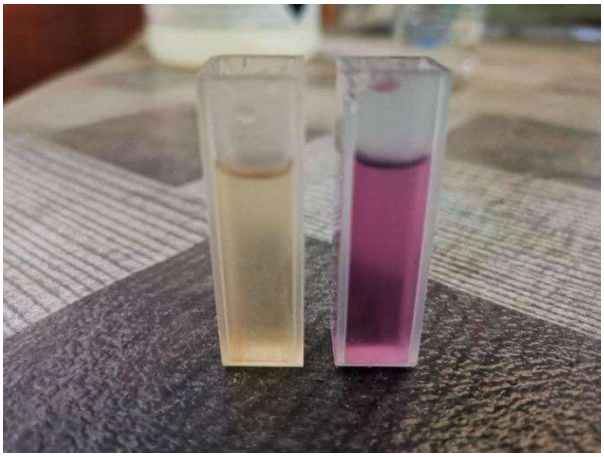

Figure 2. Change in the color of the sample from violet to yellow.

Anti-bacterial activity

Zs-c leaves CH_3OH extract anti-bacterial activity revealed variable inhibition effects against gram-positive bacteria Sa (+) and gram negative bacteria Ec (-), as show in Fig. 3, and against the two fungi An and Ca, in Fig. 4. The results are summarized in Table 4.

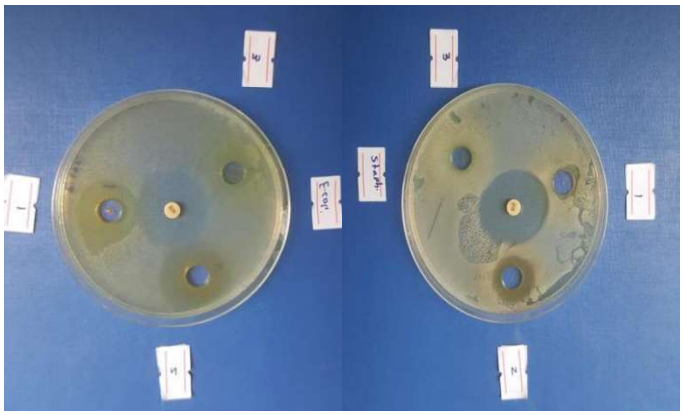

Figure 3. Effect of Zs-c leaves CH_3OH extract (no. 2) on Ec and Sa bacteria strains.

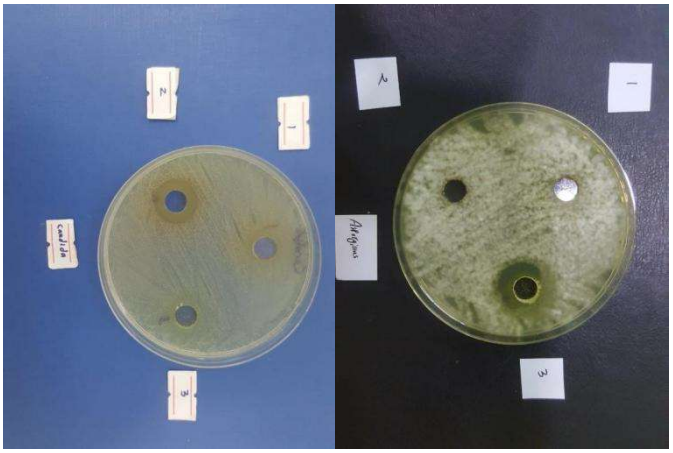

Figure 4. Effect of Zs-c leaves CH_3OH extract (no. 2) on Ca and An fungi.

Table 4. Anti-bacterial and anti-fungal activity results of Zs-c leaves CH_3OH extract.

Test organisms	Inhibition zone (mm)
Ec	27
Sa	14
Ca	18
An	-

From Table 4, Zs-c leaves CH_3OH extract showed high activity against Ec (27 mm) and Sa (14 mm). So, Zs-c leaves CH_3OH extract was more active against Gram negative bacteria (Ec) than against Gram positive bacteria (Sa). It was active for Ca and inactive for An. This result was similar to Al-Bayatti's study [28].

TPC

TPC of Zs-c leaves CH_3OH extract was notable, with the highest value of 70.06 mg GAE/g. Generally, higher TPC than TFC are logical, since the former are major polyphenol compounds. This indicates that the extract contains other phenolic compounds with different chemical structures than flavonoids (phenolic acids, tannins, etc.) [29].

Figs. 5 and 6 show $C_7H_6O_5$ standard curve and diluted concentrations, respectively.

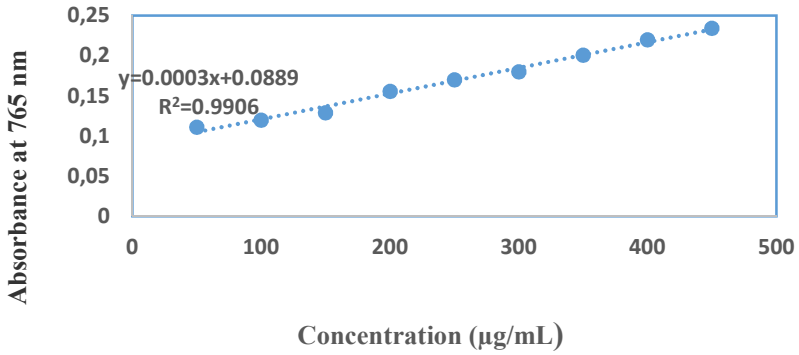

Figure 5. $C_7H_6O_5$ standard curve.

Figure 6. $C_7H_6O_5$ diluted concentrations to make TPC standard curve.

TFC

Examination of TFC results shows a positive correlation between the standard QCT concentration and the absorbance, with a R^2 value of 0.9906. Zs-c leaves CH_3OH extract showed a TFC of 25 mg QCTE/g. Figs. 7, 8 and 9 show QCT

standard curve, its diluted concentrations, and a summary of TPC and TFC for Zs-c leaves CH_3OH extract.

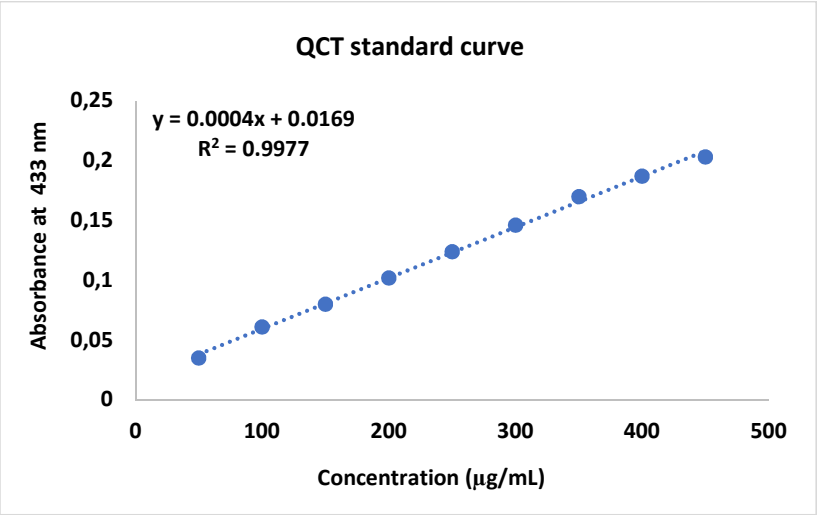

Figure 7. QCT standard curve.

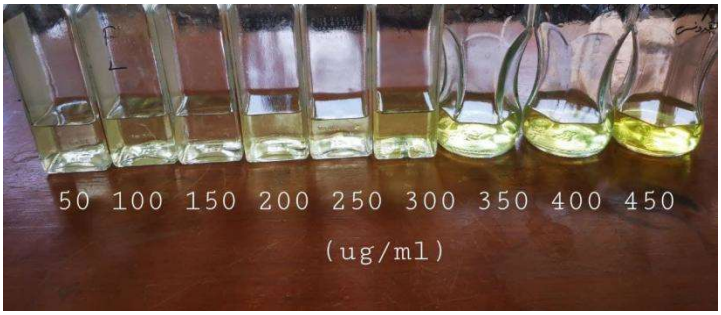

Figure 8. QCT diluted concentrations to make TFC standard curve.

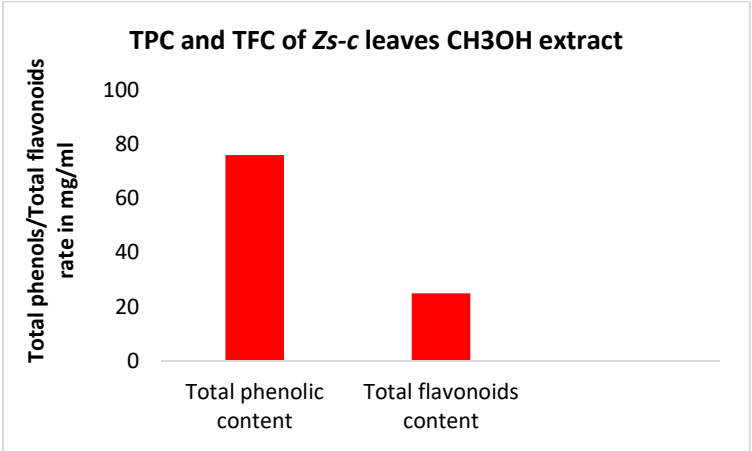

Figure 9. Summary of TPC and TFC for Zs-c leaves CH_3OH extract.

Corrosion study

Zs-c leaves CH_3OH extract was evaluated as inhibitor for C1010 alloy corrosion in 0.1 M HCl. The electrochemical data for the alloy surface, with different

CH_3OH extract concentrations, were obtained by plotting the Tafel plots, as shown in Fig. 10, and are summarized in Table 5.

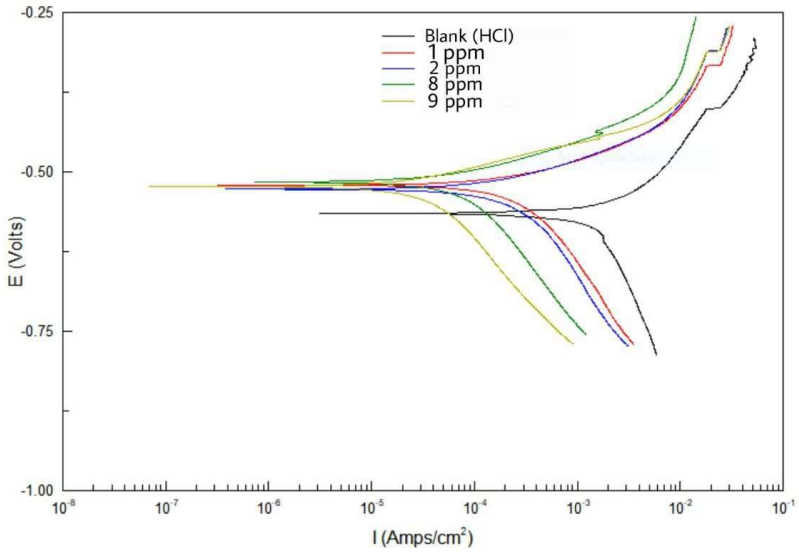

Figure 10. Tafel plots for CS alloy with different Zs-c leaves CH_3OH extract concentrations, relative to the blank solution, at 25 ºC.

Table 5 and Fig. 10 show the electrochemical data obtained from Tafel plots at 1, 2, 8 and 9 ppm concentrations of Zs-c leaves CH_3OH extract, as an anti-corrosion agent for CS in HCl. Generally, an increase in the inhibitors concentrations significantly changed the electrochemical factors obtained from the Tafel plots. It was noted that higher inhibitors concentrations led to lower I_{corr} and CR values, and increased R_p. In its turn, IE increased from 85,24%, at 1 ppm (mg/L^{-1}), to 96.06%, at 9 ppm, which was due to the inhibitor layer adsorption onto the C1010 surface. On the other hand, E_{corr} value was lower in the inhibited solution, with higher inhibitors concentrations, than in the blank solution. There was a small displacement between E_{corr} with and without inhibitor. If this difference is lower than -89 mV, it indicates that the inhibitor is of mixed type [30-31]. β_a and β_c values are shown in Table 5.

Table 5. Electrochemical data for CS alloy surface corrosion without and with Zs-c leaves CH_3OH extract, in different concentrations, at 25 ºC.

Constituent	**Conc. ppm**	**$-E_{corr}$ mV vs. SCE**	**β_a mV/decade**	**β_c mV/decade**	**R_p Ω.cm²**	**I_{corr} µA.cm-²**	**CR Mpy**	**IE %**
HCl	----	- 567	213.23	1198.36	11.471	1569.2	726.65	------
HCl + Zs-c leaves CH_3OH extract	1	- 529	87.665	322.77	77.723	231.59	107.24	85.24
	2	- 535	81.024	435.56	98.972	181.87	84.219	88.40
	8	- 517	72.171	266.07	243.78	73.83	34.192	95.29
	9	- 517	71.034	329.14	291.49	61.75	28.596	96.06

It can be noticed that those values varied with different inhibitor concentrations, which indicates changes in the inhibition mechanism. This means that the prepared inhibitors acted by simple blocking the reactions [32-33].

Study of Zs-c leaves CH_3OH extract adsorption isotherm

There are various isotherms used to determine the appropriate adsorption mechanism of inhibitors onto metals surface, such as Temkin's, Langmuir's, Frumkin's and Freundlich's isotherms. The most suitable model to describe Zs-c leaves CH_3OH extract adsorption onto the alloy surface was Langmuir's isotherm, which is shown by the following equation:

$$\frac{C_{inh}}{\theta} = \frac{1}{Kads} + C_{inh} \quad (1)$$

where C_{inh} is the inhibitor concentration in ppm [34-35]. Langmuir's adsorption isotherm was the most suitable for this inhibitor, because it gave a R^2 value close to 1 [35].

At 25 ºC (298 K), the plotting of C_{inh}/θ *vs* C_{inh} (Fig. 11) gave a straight line for K_{ads}, given by the y-intercept reciprocal, but at 35, 45 and 55 ºC (308, 318 and 328 K), it was calculated directly through equation (1), for an optimal concentration.

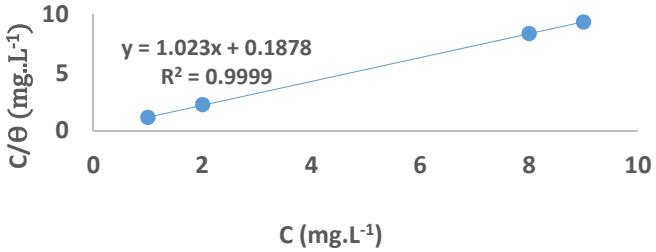

Figure 11. Langmuir's adsorption isotherm model of *Zs-c* leaves CH_3OH extract.

Thus, equation (1) can be rewritten by the following equation:

$$K_{ads} = \frac{\theta}{C - C\theta} \quad (2)$$

ΔG^o_{ads} action of the inhibitor on the alloy was calculated towards K_{ads} values, as in equation (3):

$$\Delta G°_{ads} = -RTln(55.5)K_{ads} \quad (3)$$

55.5 is the water concentration in mol/L^{-1}. Thus, equation (3) can be rewritten by the following equation:

$$\Delta G°_{ads} = -RTln(999000)K_{ads} \quad (4)$$

The above value (999000) represents the product of water concentration (55.5) and molecular weight (18 g/mol^{-1}) multiplied by 1000, to convert the unit of grams to:

$$lnK_{ads} = constant - \left(\frac{\Delta H°ads}{R}\right)\left(\frac{1}{T}\right) \quad (5)$$

By plotting InK_{ads} *vs.* 1/T, a straight line was obtained, and the given slope was $\frac{-\Delta H°ads}{R}$, as in Fig. 12. ΔS^o_{ads} was calculated according to the following equation [36]:

$$\Delta S°_{ads} = \frac{\Delta H°ads - \Delta G°ads}{T} \quad (6)$$

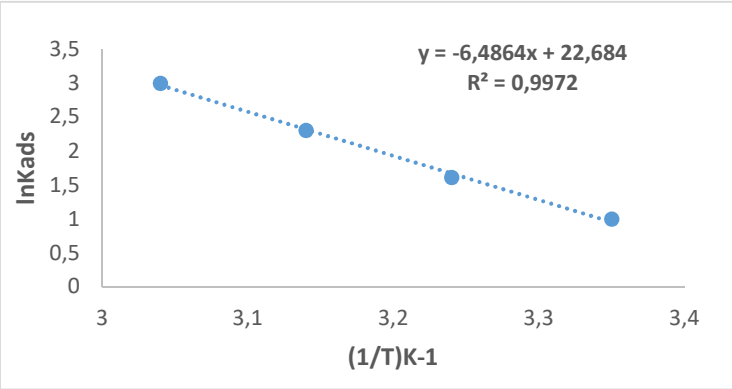

Figure 12. Calculation of ΔH^{o}_{ads} and ΔS^{o}_{ads} for the inhibitor adsorption onto the CS alloy surface.

Table 6 shows thermodynamic functions for Zs-c leaves CH_3OH extract optimum concentration (9 ppm), at all studied temperatures (from 25 to 55 ºC).

Table 6. Thermodynamic functions for Zs-c leaves CH_3OH extract at optimum concentration.

Extract	Optimum conc.	Temp. K	ΔG^{o}_{ads} kJ/mol^{-1}	ΔS^{o}_{ads} j/K^{-1}/mol^{-1}	ΔH^{o}_{ads} jK/mol^{-1}	R^2
Zs-c leaves CH_3OH extract	9	298	- 9.2716	40.3059	110.84	0.99
		308	- 7.1422	38.3059		
		328	- 1.8798	34.3657		

The effect of temperature on the corrosion reaction

The effect of temperature on the corrosion reaction without and with inhibitor, at its optimal concentration, was studied at 25 (298 K), 35 (308 K), 45 (318 K) and 55 ºC (328 K). Table 7 and Fig. 13 show that, as temperature increased, I_{corr} and CR values were higher, while R_p and IE% values were lower.

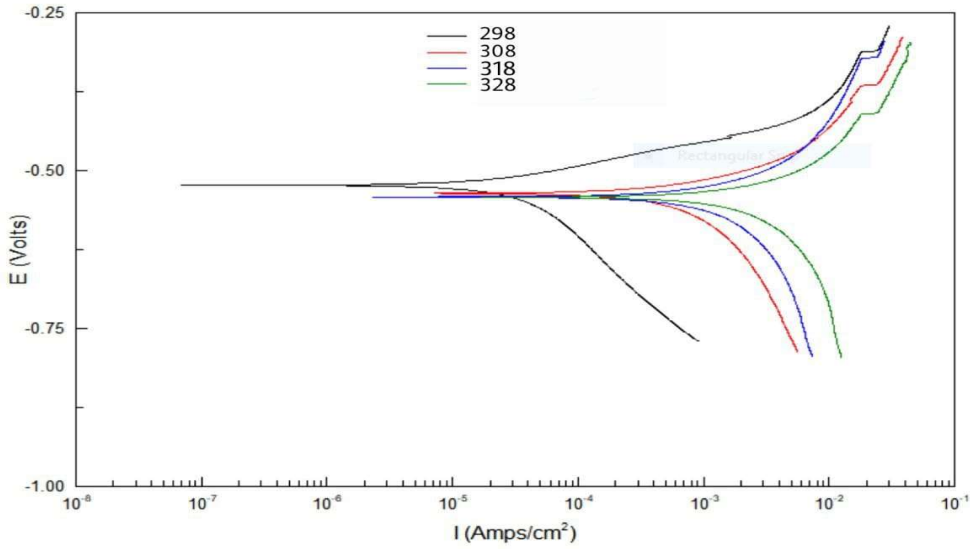

Figure 13. Tafel plots for five concentrations of Zs-c leaves CH_3OH extract, compared to the blank solution, at different temperatures.

Table 7. Electrochemical data for CS alloy surface corrosion, without and with Zs-c leaves CH_3OH extract, at different concentrations and temperatures.

Constituent	Conc. ppm	Temp. K	E_{corr} mV vs. SCE	β_c mV/decade	B_a mV/decade	R_p Ω/cm²	I_{corr} µA/cm⁻²	CR mpy	IE%
HCl (blank)		298	-567	0498.36	213.23	11.471	1596.2	726.65	
		308	-563	1179.14	283.06	10.341	1740.06	806.05	
	-	318	-571	1213	131.53	9.581	1891.12	875.75	
		328	-549	1110.3	465.17	6.533	2734.2	1266.1	
		298	-517	329.14	71.043	291.49	61.75	28.59	96.06
Zs-c leaves CH_3OH extract	9	308	-538	732.17	136.72	29.143	617.63	286.01	64.51
		318	-542	361.32	170.91	17.96	1002.2	464.1	47.00
		328	-543	2403.06	274.79	9.541	1885.8	873.27	31.02

These values can be attributed to the kinetic energy reduction for the corrosive molecules, whether without or with inhibitor [37-38]**.** In this study, to better understand C1010 corrosion reaction behavior, without and with inhibitor, kinetic parameters were calculated according to Arrhenius equation [39]:

$$\ln(CR) = \ln A - \frac{E_a^*}{RT} \qquad (7)$$

where A is Arrhenius factor (s^{-1}), T is absolute temperature (K) and R is the universal gas constant (8.314 kJ^{-1}/mol^{-1}).

By plotting the above relationship, i.e., ln(CR) against 1/T, E_a^* was calculated as in Figs. 14 and 15.

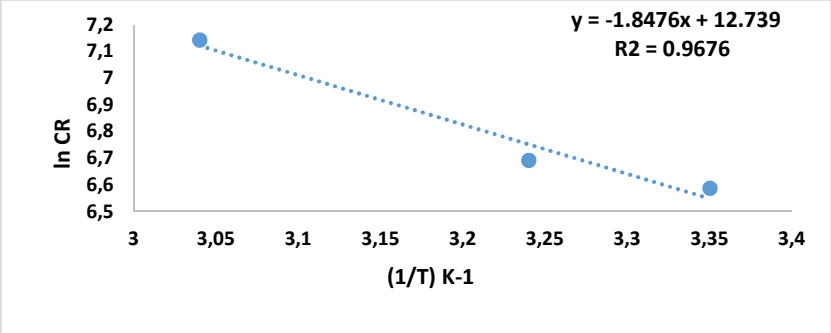

Figure 14. E_a^* calculation for CS alloy corrosion reaction without inhibitor.

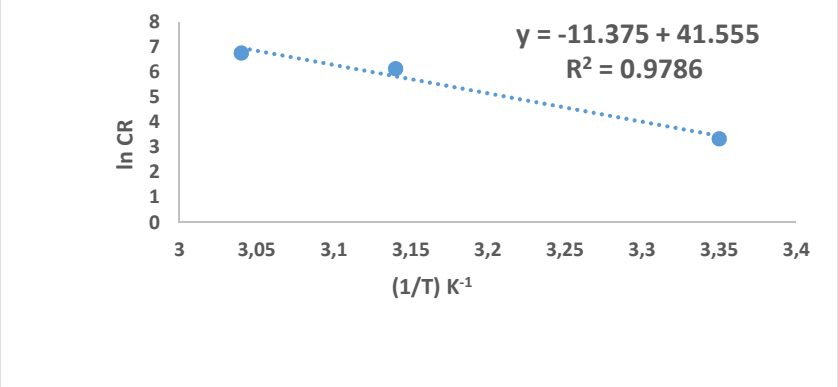

Figure 15. E_a^* calculation for CS alloy corrosion reaction with inhibitor.

On the other hand, other kinetic parameters, such as ΔH^*, ΔS^* and ΔG^*, were calculated, where the first two were estimated according to the following equation [30][37]:

$$\ln\left(\frac{CR}{T}\right) = [\ln(\frac{R}{Nh}) + \frac{\Delta S^*}{R}] - \frac{\Delta H^*}{RT} \quad (8)$$

where N is Avogadro's number (6.023 x 10^{23} mol^{-1}) and h is the Plank's constant that is equal to 6.625 x 10^{-34} J/s. By plotting $\ln\left(\frac{CR}{T}\right)$ against $\frac{1}{T}$, the slope is equal to $\frac{-\Delta H^*}{R}$, and the intercept is equal to $\ln[(\frac{R}{Nh}) + \frac{\Delta S^*}{R}]$, as in Figs. 16 and 17.

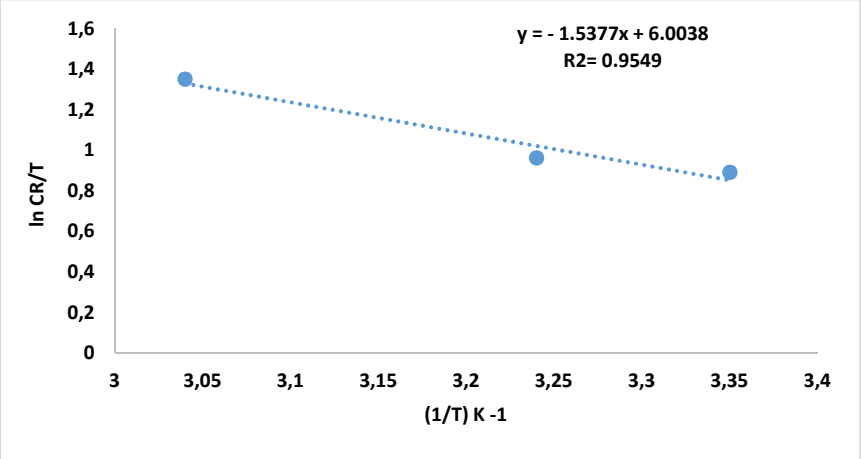

Figure 16. Calculation of ΔH and ΔS for CS without inhibitor.

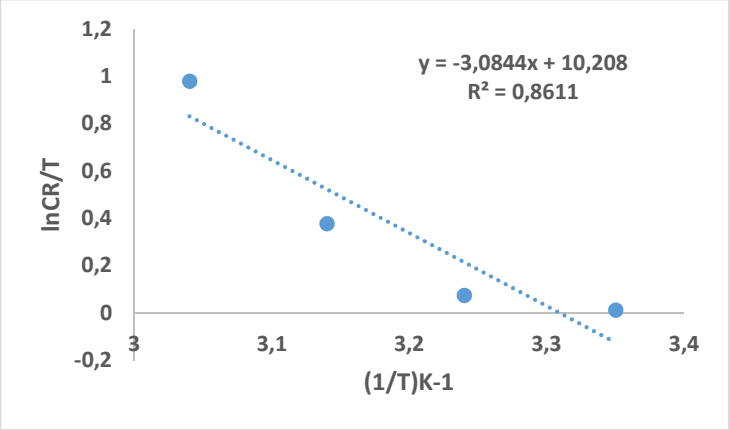

Figure 17. Calculation of ΔH and ΔS for CS with inhibitor.

Thus, kinetic parameters data can be summarized in Table 8.

Table 8. Kinetic parameters for CS alloy corrosion reaction without and with inhibitor, at optimal concentration.

Comp.	Conc.	E_a kJ/mol^{-1}	A s^{-1}	ΔH kJ/mol^{-1}	ΔS J/k/mol^{-1}
HCl	-------	15.36	3.4078 x 10^5	12.78	-91.62
CH_3OH extract	9 ppm	94.57	1.1145 x 10^{18}	92.00	91.98

Table 8 reveals that E_a^* increased more with the extract, which means that C1010 corrosion reaction with the inhibitor was lower than without it. E_a^* values were 15.36 and 94.57 kJ/mol^{-1}, without and with inhibitor, respectively, which is higher than the threshold value of 80 kJ/mol^{-1} required for chemisorption.
Thus, it is concluded that the inhibitor underwent chemical adsorption. This higher E_a^* value with the inhibitor is attributed to an appreciable decrease in the HCl molecules adsorption onto the alloy surface [40].
The corresponding increase in the corrosion rate is also attributed to the greater metal area exposed to HCl. ΔH* positive sign refers to the endothermic nature of the dissolution process, whether without or with the inhibitor, which implies that the alloy dissolution increased with higher temperatures, but it became difficult in the inhibitor presence [41-42].
The Arrhenius factor depicted that the corrosive molecules vibration increased with the inhibitors. In other words, these corrosive molecules will be mixed with the inhibitor molecules, to form a stable film on the surface alloy. ΔS value was negative without inhibitor, because the corrosive molecules tended to be stable after they have reacted with the alloy surface with inhibitor. With the extract, ΔS value was positive, since the inhibitor molecules incorporated within the corrosive molecules, forming a protective film on the alloy surface, and the activated complex was formed as a rate determining step [43].

Conclusions

Several points can be summarized below as conclusions:

1- Zs-c leaves CH_3OH extract showed high efficiency as an inhibitor for C1010 corrosion, with an IE of 96.06%, at 9 ppm, at 25 ºC, in 0.1 M HCl.
2- IE% decreased with increasing temperatures.
3- The inhibitor showed TPC of 70 mg GAE/G and TFC of 25 mg QCTE/g.
4- The extract showed high IE% values against Sa + (inhibition diameter of 17 mm) and Ec - bacteria (inhibition diameter of 27 mm) growth, with 100 mg/mL.
5- The inhibitor showed IE% values against Ca fungi growth (inhibition of 18 mm), but it had no effect on An fungi.
6- The inhibitor contributed to increase E_a^* of C1010 corrosion reaction, and it behaved as an anodic inhibitor.

Authors' contributions

Sarah Z. AL-Ashoor (M.Sc. student): conceived and designed the analysis; collected the data. **Dawood S. Ali (1st Sarah's supervisor)**: inserted data or analysis tools. **Hadi Z Al-Sawaad (2nd Sarah's supervisor)**: performed the analysis; wrote the paper.

Abbreviations

$AlCl_3$: aluminum trichloride
An: *Aspergillus niger*
Ca: *Candida albicans*
C_6H_6O: phenol
$C_7H_6O_5$: gallic acid

CE: counter electrode
CH_3OH: methanol
CR: corrosion rate
CS: carbon steel
DMSO: dimethyl sulfoxide
DPPH: 2,2-diphenyl-1-picrylhydrazyl
E: electric potential
Ec: *E. coli*
E_{corr}: corrosion potential
FCR: *Folin-Ciocâlteu* reagent
HCl: hydrochloric acid
HE: hydroethanolic acid
IC_{50}: half-maximal inhibitory concentration
I_{corr}: corrosion current density
J: current density
IE%: inhibition efficiency
mg GAE/g: milligrams of gallic acid equivalent per gram
mg QCTE/g: milligrams of quercetin equivalent per gram
Na_2CO_3: sodium carbonate
OCP: open circuit potential
PDA: potato dextrose agar
PDP: potentiodynamic polarization
QCT: quercetin
R^2: correlation coefficient
RE: reference electrode
R_p: polarization resistance
Sa: *Staphylococcus aureus*
SC*:* scan rate
TEB: tebuconazole
TFC: total flavonoid contents
TPC: total phenolic contents
WE: working electrode
Zs-c*: Ziziphus spina-christi*

Symbols definition
βa: anodic Tafel slope
βa: cathodic Tafel slope
ΔG_{ads}: adsorption free energy
ΔH_{ads}: adsorption enthalpy
ΔS_{ads}: adsorption entropy
E_a^*: activation energy
K_{ads}: adsorption equilibrium constant (L/mg^{-1})
θ: surface coverage

References

1. Nazif NM. Phytoconstituents of *Zizyphus spina-christi* fruits and their antimicrobial activity. Food Chem. 2002(76)1:77-81. https://doi.org/10.1016/S0308-8146(01)00243-6
2. Yossef H, Khedr AA, Mahran MZ. Hepatoprotective activity and antioxidant effects of *El Nabka* (*Zizyphus spina-christi*) fruits on rats hepatotoxicity induced by carbon tetrachloride. Nat Sci. 2011;9(2). http://www.sciencepub.net/nature 2011
3. Abalaka M, Daniyan SY, Mann A. Evaluation of the antimicrobial activities of two *Ziziphus* species (*Ziziphus mauritiana* L. and *Ziziphus spinachristi* L.) on some microbial pathogens. Afr J Pharm Pharmacol. 2010;(4)4:135-139. https://doi.org/10.5897/AJPP.9000150
4. Almeer RS, El-Khadragy MF, Abdelhabib S et al. *Ziziphus spina-christi* leaf extract ameliorates schistosomiasis liver granuloma, fibrosis, and oxidative stress through down regulation of fibrinogenic signaling in mice. PLoS One. 2018;(13)10. https://doi.org/10.1371/journal.pone.0204923
5. Asgarpanah J, Khoshkam R. Phytochemistry and pharmacological properties of *Ruta graveolens* L. J Med Plants Res. 2012:6(23):3942-3949. https://doi.org/10.5897/JMPR12.040
6. Abdoul-Azize S. Potential Benefits of Jujube (*Zizyphus Lotus*) L. Bioactive Compounds for Nutrition and Health. J Nutr Metab. 2016. https://doi.org/10.1155/2016/2867470
7. Okewale A. The Use of Rubber leaf Extract as a Corrosion Inhibitor for Mild Steel in Acidic Solution. Int J Mater Chem. 2017;(7)1:5-13. https://doi.org/10.5923/j.ijmc.20170701.02
8. Divya G, Sathiya M, Mary AC. Inhibition of corrosion of carbon steel in aqueous medium using naval leaf extract. Int J Res Chem Environ. 2016;(6)1:1-7. www.ijrce.org
9. Harnsoongnoen S, Siritaratiwat A, Szymońska J et al. Characterization of starch nanoparticles. J Phys: Conf Ser. 2009;146:012027. https://doi.org/10.1088/1742-6596/146/1/012027
10. Hansson CM. The impact of corrosion on society. Metall Mater Trans. 2011;(42)10: 2952-2962. https://doi.org/10.1007/S11661-011-0703-2
11. Laamari R, Benzakour J, Berrekhis F et al. Corrosion inhibition of carbon steel in hydrochloric acid 0.5 M by hexa methylene diamine tetramethyl-phosphonic acid. Arab J Chem. 2011;(4)3:271-277. https://doi.org/10.1016/J.ARABJC.2010.06.046
12. Shaw B, Kelly R. What is Corrosion? Electrochem Soc Interface. 2006;(15)1:24. https://doi.org/10.1149/2.F06061IF
13. Ingle K, Deshmukh A, Padole DA et al. Phytochemicals: Extraction methods, identification and detection of bioactive compounds from plant extracts. J Pharmacog Phytochem. 2017;(6)1:32-36. https://doi.org/10.22271/phyto B
14. Owolarafe TA, Salau AK, Salawu K. Phytochemical screening and toxicity study of aqueous-methanol extract of *Ziziphus spina-christi* seeds in Wistar albino rats. Comp Clin Path. 2020;(29)1:267-274 https://doi.org/10.1007/S00580-019-03043-5
15. V. Singh, Kumar R. Study of phytochemical analysis and antioxidant activity of *Allium sativum* of Bundelkhand region. Int J Life Sci Res. 2017; 3(6):1451-1458. https://doi.org/10.21276/ijlssr.2017.3.6.4
16. Tiwari P, Kaur H, Kaur M. Phytochemical screening and Extraction: A Review. Int Pharm Sci. 2011;1:98-106.
17. N. Raaman N. Qualitative phytochemical techniques. Phytochem Tech. 2006: 19-24.

18. Dangoggo S, Hassan L, Sadiq SI et al. Phytochemical analysis and antibacterial screening of leaves of *Diospyros mespiliformis* and *Ziziphus spina-christi*. J Chem Eng. 2012;(1)1:31-37. https://doi.org/10.1.1.1091.1095
19. Pambudi D, Fajriyah NN, Shalekhah VR. Test on the Antioxidant Activities of Methanol Extract of Bidara Leaves (*Ziziphus spina-christi*) using the DPPH Radical Immersion Method. Borneo J Pharm. 2020;3(1):44-51. https://doi.org/10.33084/bjop.v3i1.1242
20. Bukar AM, Kyari MZ, Gwaski PA et al. Evaluation of phytochemical and potential antibacterial activity of *Ziziphus spina-christi* L. against some medically important pathogenic. J Pharmacogn Phytochem. 2015;3(5):98-101.
21. Talibi I, Askarne L, Boubaker H et al. Antifungal activity of some Moroccan plants against *Geotrichum candidum*, the causal agent of postharvest citrus sour rot. Elsevier. 2012;(35):41-46. https://doi.org/10.1016/j.cropro.2011.12.016.
22. A. Dehpour, Fazel NS, Ebrahimzadeh MA et al. Antioxidant activity of the methanol extract of *Ferula assafoetida* and its essential oil composition. Grasas y Aceites. 2009;60(4):405-412. https://doi.org 10.3989/gya.010109
23. Djeridane A, Yousfi M, Nadjemi B et al. Antioxidant activity of some Algerian medicinal plants extracts containing phenolic compounds. Elsevier. 2006;(97)4:654-660. https://doi.org/10.1016/j.foodchem.2005.04.028
24. B. Vyas, Hansson ILH. The cavitation erosion-corrosion of stainless steel. Corros Sci. 1990;(30)8-9:761-770. https://doi.org/10.1016/0010-938X(90)90001-L
25. Najafabad A, Jamel R. Free radical scavenging capacity and antioxidant activity of methanolic and ethanolic extracts of plum (*Prunus domestica L.*) in both fresh and dried samples. Avicenna J Phytomed. 2014;4(5):343-53. https://doi.org/10.22038/ajp.2014.2827
26. Rahman MM, Islam MB, Biswas M et al. In vitro antioxidant and free radical scavenging activity of different parts of *Tabebuia pallida* growing in Bangladesh. BMC Res Notes. 2015;(8)1. https://doi.org/10.1186/S13104-015-1618-6
27. Akar Z, Küçük M, Doğan H. A new colorimetric DPPH scavenging activity method with no need for a spectrophotometer applied on synthetic and natural antioxidants and medicinal herbs. J Enzyme Inhib Med Chem. 2017;32(1):640-647. https://doi.org/10.1080/14756366.2017.1284068
28. Al-Bayatti K, Aziz MF, Abdalah ME. A Study of Antibacterial Activity of Cidar (*Zizyphus spinachristi* L.) on Bacterial Pathogens isolated from Skin Infections. AJPS. 2011;(9)1. http://ajps.uomustansiriyah.edu.iq/index.php/AJPS/article/view/268
29. Bakchiche B. Activités antioxydantes des polyphenols extraits de plantes médicinales de la pharmacopée traditionnelle d'Algérie [Antioxidant activities of polyphenol extracts]. Int J Innov Appl Stud. 2014(9)1;167-172. https://doi.org/10.1.1.686.4147
30. Radey H, Khalaf M, Al-Sawaad HZ. Novel Corrosion Inhibitors for Carbon Steel Alloy in Acidic Medium of 1 N HCl Synthesized from Graphene Oxide. Open J Org Polym Mat. 2018;(8)4. https://doi.org/ 0.4236/ojopm.2018.84005
31. Manssouri M, El Ouadi Y, Znini M et al. Adsorption proprieties and inhibition of mild steel corrosion in HCl solution by the essential oil from fruit of *Moroccan ammodaucus leucotrichus*. J Mater Environ Sci. 2015;(6)3:631-646.

32. Loto RT, Loto C. Effect of P-phenylediamine on the corrosion of austenitic stainless steel type 304 in hydrochloric acid. Int J Electrochem Sci. 2012;(7)10:9423-9440.
33. Serrar H, Laroujb M, Gazb HL et al. Experimental and Theoretical Studies of the Corrosion Inhibition of 4-amino-2-(4-chlorophenyl)-8-(2, 3-dimethoxyphenyl)-6-oxo-2, 6-dihydropyrimido [2, 1-b][1, 3] thiazine-3,7-dicarbonitrile on Carbon Steel in a 1.0 M HCl Solution. Port Electrochim Acta. 2018;36(1):35-52. https://doi.org/10.4152/pea.201801035
34. Lebrini M, Robert F, Roos C. Adsorption properties and inhibition of C38 steel corrosion in hydrochloric solution by some indole derivates: temperature effect, activation energies. Int J Corros. 2013. https://doi.org/10.1155/2013/139798
35. Juhaiman LAA, Mustafa AA, Mekhamer WK. Polyvinyl pyrrolidone as a green corrosion inhibitor for carbon steel in alkaline solutions containing NaCl. Anti-Corros Meth Mater. 2013;(60)1:28-36. https://doi.org/10.1155/2013/139798
36. Ostovari A, Hoseinieh S, Peikari M. Corrosion inhibition of mild steel in 1 M HCl solution by henna extract: A comparative study of the inhibition by henna and its constituents (Lawsone, Gallic acid, α-d). Corros Sci. 2009;(51)9: 1935-1949. https://doi.org/10.1016/j.corsci.2009.05.024
37. Al-Sawaad HZ, Faili N, Essa AH. Evaluation of Vicine as a Corrosion Inhibitor for Carbon Steel Alloy. Port Electrochim Acta. 2019;37(4):205-216 https://doi.org/10.4152/pea.201904205
38. Okafor PC, Osabor VI, Ebenso EE. Eco-friendly corrosion inhibitors: Inhibitive action of ethanol extracts of *Garcinia kola* for the corrosion of mild steel in H2SO4 solutions. Pigm Res Technol. 2007;(36)5:299-305. https://doi.org/10.1108/03699420710820414
39. Khadom AA. Effect of temperature on corrosion inhibition of copper-nickel alloy by tetraethylenepentamine under flow conditions. J Chil Chem. Soc. 2014:59(3). https://doi.org/10.4067/S0717-97072014000300004
40. Al-Jubanawi I, Al-Sawaad HZ, Al-Waaly A. *Bis thiourea phthalato* Cobalt (II) complex: synthesis and studying as corrosion inhibitors for carbon steel alloy (C1010) in 0.1 M HCl. J Mater Environ Sci. 2020;8:1386-1402. https://doi.org/10.3103/S1068375521050057
41. Larouj M, Ourrak K, El M'Rabet M. Thermodynamic study of corrosion inhibition of carbon steel in acidic solution by new pyrimidothiazine derivative. J Mater Environ Sci. 2017;8(11):3921-3931.
42. Kairi N, Kassim J. The effect of temperature on the corrosion inhibition of mild steel in 1 M HCl solution by *Curcuma longa* extract. Int. J. Electrochem. Sci. 2013;8:713-7155.
43. Prasanna B, Praveen B, Hebbar N. Electrochemical study on inhibitory effect of Aspirin on mild steel in 1 M hydrochloric acid. Elsevier. 2017;(22)62-69. https://doi.org/10.1016/j.jaubas.2015.11.001